

COMPUTATIONALLY EFFECTIVE DISCONTINUOUS GALERKIN SCHEME FOR LINEARIZED EULER EQUATIONS

Vladimir Vlasenko*, Andrey Wolkov** and Charles Hirsch***

**Central Aerohydrodynamic Institute (TsAGI)
Zhukovsky street, 1, 140185 Zhukovsky,
Moscow Region, Russian Federation,
Email: vvylas@pt.comcor.ru*

***Central Aerohydrodynamic Institute (TsAGI)
Zhukovsky street, 1, 140185 Zhukovsky,
Moscow Region, Russian Federation,
Email: andrey.wolkov@mail.ru*

****NUMECA International, Avenue Franklin Roosevelt, 5,
1050 Brussels, Belgium,
Email: charles.hirsch@numeca.be*

Key words: aeroacoustics, Discontinuous Galerkin, linearized Euler Equations, Riemann problem, Roe linearization, isentropic perturbations, Gaussian acoustic pulse.

Abstract. The family of DG methods for solution of Linearized Euler Equations (LEE) is considered. For model advection equation, comparison of various DG schemes and finite-volume schemes is performed. Realization of Roe solver of Riemann problem for LEE is investigated. The following possibilities to increase the effectiveness of Riemann solver are considered: 1) to solve one Riemann problem with the same Roe matrix as for full Euler equations; 2) to replace Roe averagings by simple arithmetic mean; 3) to formulate task in primitive variables instead of conservative variables. Applicability range of these simplifications is found. The final simplification is the use of Isentropic LEE. Finally, DG schemes are applied to test task about development of Gaussian acoustic pulse in a uniform flow.

1. INTRODUCTION

This works considers the problems of computationally effective realization of Discontinuous Galerkin (DG) approach for numerical solution of aeroacoustic tasks.

Acoustic tasks are characterized by the necessity to simulate propagation of very small perturbations over non-uniform aerodynamic flowfields. This implies that numerical method should handle multiscale tasks with low dispersion and low dissipation errors for small scales. This requirement leads necessarily to high-order numerical schemes. In addition, very detailed numerical grids and rather large computational domains should be considered to calculate accurately the near acoustic field and to have possibility to impose correctly boundary conditions for calculations of the far acoustic field.

Discontinuous Galerkin finite-element numerical methods¹ have many attractive properties:

– it is easy to design a scheme with any prescribed order of accuracy in space and time;

– DG approach allows an easy use of adaptivity strategies, since refinement or unrefinement of the mesh can be achieved without taking into account of the continuity restrictions characteristic for other finite-element methods;

– DG is an explicit method, allowing very efficient time-marching calculations;

– DG methods combines attractive properties of finite-element methods (easy handling of complicated geometry) with attractive properties of finite-volume methods (high resolution for discontinuous solutions due to using monotone fluxes or approximate Riemann solvers applied at the element interfaces and limiters);

– so far DG is the only class of high order methods, for which it is possible to prove cell entropy inequalities for any scalar nonlinear conservation laws in any spatial dimensions and for any order of accuracy, even without the need of nonlinear limiters;

– DG approach produces highly compact schemes: the evolution of information in any element depends only on the information of itself and its immediate neighbors, regardless of the order of accuracy. As a result, it allows very efficient parallel implementation.

DG approach is very attractive for acoustic calculations, because it allows constructing high-accuracy scheme with compact stencil, very useful for massive parallel computations. DG approach is widely used in aeroacoustic calculations^{2,3}.

In this paper the properties of a family of DG schemes for Linearized Euler Equations are considered, and possibilities to improve their computational efficiency are investigated.

2. FAMILY OF DISCONTINUOUS GALERKIN SCHEMES FOR LINEARIZED EULER EQUATIONS

2.1. Linearized Euler Equations

Let's consider Euler equations in conservative form:

$$\frac{\partial \mathbf{U}}{\partial t} + \nabla \cdot \vec{\mathbf{F}}(\mathbf{U}) = 0, \quad (1)$$

where $\mathbf{U} = [\rho; \rho u; \rho v; \rho w; \rho E]^T$ is vector of conservative variables (values of mass, x-momentum, y-momentum, z-momentum and energy per unit volume of gas), $\vec{\mathbf{F}}(\mathbf{U})$ - fluxes of \mathbf{U} along Cartesian axes. E is total energy per unit mass of gas: $E = \frac{1}{2}(u^2 + v^2 + w^2) + \frac{1}{\gamma - 1} \frac{p}{\rho}$ (γ is specific heat ratio that is supposed to be constant).

We shall suppose that there is basic *aerodynamic* flowfield with static pressure $p_a(x, y, z)$, with velocity $u_{ai}(x, y, z)$ ($i = 1, 2, 3$) and with density $\rho_a(x, y, z)$. This field itself satisfies Euler equations. Then we consider small non-stationary perturbations on the background of this stationary basic flowfield: $\rho = \rho_a + \rho'$, $u_i = u_{ai} + u'_i$, $p = p_a + p'$. We shall assume that these perturbations are small in comparison with basic parameters:

$|\rho'| \ll |\rho_a|$, $|u'_i| \ll |V_a|$ ($V_a = \sqrt{u_a^2 + v_a^2 + w_a^2}$), $|p'| \ll |p_a|$. Then these perturbations satisfy to Linearized Euler Equations (LEE):

$$\frac{\partial U'}{\partial t} + \nabla \cdot \vec{F}'(U', U_a) = 0. \quad (2)$$

In this system, vector $U' = [U'_1; U'_2; U'_3; U'_4; U'_5]^T$ consists of perturbations of Euler conservative variables. We use formulation of (2) in primitive variables:

$$\Gamma \frac{\partial Q'}{\partial t} + \nabla \cdot \vec{F}'(U', U_a) = 0, \quad (3)$$

where $Q' = (\rho', u', v', w', p')^T$ and $\Gamma = \begin{pmatrix} \partial U' \\ \partial Q' \end{pmatrix}$.

Flux of U' per unit area in direction of the vector $\vec{n} = (n_x, n_y, n_z)$ (*outward unit normal to the element of the control volume surface*) is equal to

$$F'_n(U', U_a) \equiv \vec{F}'(U', U_a) \cdot \vec{n} = \begin{pmatrix} D'_n \\ u_a D'_n + (U'_2 - u_a U'_1) V_{an} + p' n_x \\ v_a D'_n + (U'_3 - v_a U'_1) V_{an} + p' n_y \\ w_a D'_n + (U'_4 - w_a U'_1) V_{an} + p' n_z \\ H_a D'_n + (U'_5 - H_a U'_1 + p') V_{an} \end{pmatrix}, \quad (4)$$

where $V_{an} = u_a n_x + v_a n_y + w_a n_z$ is projection of the basic flow velocity on vector \vec{n} , $V'_n = u'_n n_x + v'_n n_y + w'_n n_z$ - projection of velocity perturbation on this vector, $D'_n = U'_2 n_x + U'_3 n_y + U'_4 n_z = \rho_a V'_n + \rho' V_{an}$, and $H_a = E_a + p_a / \rho_a$ is total enthalpy per unit mass of gas for basic flow.

2.2. Family of DG schemes for LEE

The numerical solution of (3) for each perturbed primitive variable is represented in each cell of computational grid by linear combination of basic functions $\phi_i(x, y, z)$:

$$Q'(t, x, y, z) = \sum_{j=1}^{Kcf} u'_j(t) \phi_j(x, y, z) \quad (5)$$

where $u'_j(t)$ are the expansion coefficients to be defined, Kcf – the number of basic functions. Basic functions are polynomials: $\phi_0 = 1$; $\phi_{2-4} = (x_i - x_{0i})$; $\phi_{5-10} = (x_i - x_{0i})(x_j - x_{0j})$. Here $x_1 = x$, $x_2 = y$, $x_3 = z$ and $(x_0; y_0; z_0)$ is the center of the hexahedral computational cell, where the basic functions are defined. $Kcf = (K+1)(K+2)(K+3)/6$, where K is the maximum order of polynomial. In present investigation K varies in the range from 0 to 2, and Kcf is obtained from 1 up to 10 correspondingly. By multiplication of the residual by each trial function ϕ_i and integrating by parts over each cell, one obtains

$$\frac{d}{dt} \int_{\Omega} \varphi_i \Gamma Q' d\Omega + \oint_S \varphi_i \vec{F}'(Q', Q_a) \cdot d\vec{S} - \int_{\Omega} \vec{\nabla} \varphi_i^E \vec{F}'(Q', Q_a) d\Omega = 0, \quad i = 1, \dots, K_{cf}. \quad (6)$$

Here $d\vec{S}$ is an element of the cell surface multiplied on outward unit normal $\vec{n} = (n_x, n_y, n_z)$, and $d\Omega$ is an element of the cell volume. Aerodynamic field is also represented as

$$Q_a(t, x, y, z) = \sum_{j=1}^{K_{cf}} u_{a,j}(t) \varphi_j(x, y, z). \quad (7)$$

Surface integrals are defined using Gauss quadratures – 3 nodes per triangle for $K=1$ and 6 nodes for $K=2$. For definition of volume integrals, Quadrature-Free approach⁴ was used. Each component of LEE fluxes \vec{F}' is represented by linear combination of basic functions: $F'(Q', Q_a) = \sum_{j=1}^{F_{cf}} f_j \varphi_j^E$. Coefficients f are presented as nonlinear combination of coefficients from expression (5) and (7). After disregarding of variation of matrix Γ within cell, the system (6) is converted to the system of nonlinear equations for definition of expansion coefficients $u'_j(t)$:

$$\frac{du'_j}{dt} = \Gamma^{-1} M^{-1} \left[\int_{\Omega_E} \vec{\nabla} \varphi_j \vec{F}' d\Omega - \oint_S \varphi_j \vec{F}' d\vec{S} \right], \quad (8)$$

where M is the mass matrix: $M_{ij} = \int_{\Omega} \varphi_i^E \varphi_j^E d\Omega$.

For calculation of fluxes through the cell boundaries in the integral $\oint_S \varphi_j \vec{F}' d\vec{S}$, Riemann problem solution is used. Problems with its realization will be described in details below.

The following variants of time integration schemes were considered: 1) basic 2nd order DG scheme (**K=1, Method 1**); 2) 2nd order DG scheme with TVD method (**K=1, Method 2**); 3) basic 3rd order DG scheme (**K=2, Method 1**); 4) 3rd order DG scheme with TVD method (**K=2, Method 2**).

Basic DG schemes use 5-stage Runge-Kutta time discretization. Equation is represented as $\frac{dU'}{dt} = \text{RES}(U')$ and integrated as follows:

$$\begin{cases} U'^{(0)} = U'^n, \\ U'^{(i)} = U'^n - \alpha_i \Delta t \text{RES}(U'^{(i-1)}), \quad i = 1, \dots, 5, \\ U'^{n+1} = U'^{(5)}, \end{cases} \quad (9)$$

where n is number of time step and coefficients of the Runge-Kutta procedure are equal to $\alpha_1=0.0695$, $\alpha_2=0.1602$, $\alpha_3=0.2898$, $\alpha_4=0.5060$, $\alpha_5=1$.

DG schemes with TVD method were proposed by B.Cockburn¹. 2nd order scheme (**K=1, Method 2**) is stable for CFL number $\text{CFL} \leq \text{CFL}_{\max} = 0.333$, 3rd order scheme (**K=2,**

Method 2) – for $CFL \leq CFL_{\max} = 0.25$. This scheme includes special TVD Runge-Kutta time step integration:

$$\begin{cases} U^{(0)} = U^n, \\ U^{(i)} = \sum_{\ell=0}^{i-1} \{ \alpha_{i\ell} U^{(\ell)} + \beta_{i\ell} \Delta t \cdot \text{RES}(U^{(\ell)}) \}, \quad i = 1, \dots, K+1, \\ U^{n+1} = U^{(5)}. \end{cases} \quad (10)$$

Coefficients of the Runge-Kutta procedure are given in the Table 1.

Order	$\alpha_{i\ell}$			$\beta_{i\ell}$		
2	1			1		
	1/2	1/2		0	1/2	
3	1			1		
	3/4	1/4		0	1/4	
	1/3	0	2/3	0	0	2/3

Table 1. Runge-Kutta time discretization parameters for DG schemes with TVD method

3. COMPARISON OF DG SCHEMES WITH FINITE_VOLUME SCHEMES

To demonstrate specific properties of DG finite-element schemes in comparison with finite-volume schemes, scalar linear model equation (advection equation) may be used:

$$\frac{\partial u'}{\partial t} + u_a \frac{\partial u'}{\partial x} = 0, \quad u_a = \text{const}. \quad (11)$$

For “aerodynamic” field, we took $u_a = \text{const} = 300$. At initial time moment, we imposed small (“sound”) perturbation along the whole length of computational domain:

$$u'(x) = 0.05 \sin\left(\frac{2\pi x}{\lambda}\right), \quad \lambda = 16. \quad \text{Calculation was performed up to the moment } t = 2.5.$$

Uniform computational grid is used.

We have applied different numerical schemes to solution of this test task. From the one side, we have considered four DG schemes that were described in the section 2.2. From the other side, we have taken two well-known finite-volume schemes: 1) Godunov-Kolgan-Rodionov (GKR) scheme⁵ – typical TVD-scheme that is based on Riemann problem solution and has 2nd approximation order both in space and in time; 2) low-dissipation and low-dispersion central-difference Tam scheme with 4-step Runge-Kutta time integration (LDDRK)⁶ – classical finite-volume scheme for aeroacoustics that has 4th approximation order in space and 2nd order in time.

In Fig.1 we present the results of test computations with the use of two finite-volume schemes for different values of grid step in space h and of stability coefficient

$$C_{\text{stab}} = \frac{CFL}{CFL_{\max}}, \quad \text{where } CFL = u_a \frac{\Delta t}{\Delta x} - \text{Courant number, } CFL_{\max} \text{ is maximal Courant}$$

number, for which the scheme is stable (for GKR scheme $CFL_{\max} = 1$, for LDDRK

scheme $CFL_{\max} = 0.73$). In Fig.1,a the case is considered, when $C_{\text{stab}} = 0.5$, and when we have 8 grid cells per the wavelength of perturbation ($\lambda = 8\Delta x$). It is seen that grid resolution is deficient: in the use of all three schemes, the amplitude of perturbation is damped too strongly by scheme's numerical dissipation. If one makes grid 2 times more dense ($\lambda = 16\Delta x$), then quality of results becomes much better - see Fig.1,b. LDDRK schemes produce decrease of amplitude only by 14%, GKR scheme – by 36%. These results are not bad; but we obtain such quality, only when the stability coefficient is close to unity. If, for example, one takes $C_{\text{stab}} = 0.1$ (Fig.1,c), then the results become unacceptable again: amplitude of perturbation decreases approximately 2 times.

Therefore, in the case of finite-volume methods, the following requirements should be satisfied to obtain the enough quality of simulation of small sound perturbations: 1) it is recommended to perform calculations on the grid with no less than 16 cells per wavelength; 2) stability coefficient should belong to the range $C_{\text{stab}} \in [0.5; 1]$. The latter property is very inconvenient, because in calculations of real aircraft configurations strongly non-uniform grids are inevitable, and this fact leads to $C_{\text{stab}} \ll 1$ in smallest cells.

Results of test calculations with the use of DG schemes are presented in Fig.2,a-d.

On the first two pictures (a,b) the grid with 16 cells per wavelength is considered. Fig.2,a deals with the basic 2nd order scheme ($K=1$, Method 1). *Contrary to finite-volume schemes, quality of results increases with diminishing of C_{stab}* . Solution for $CFL = 1$ is unacceptable (amplitude is decreased nearly 2.5 times, large phase errors). Solution for $CFL = 0.5$ is better. The best results were obtained for $CFL = 0.1$. Though for $CFL \leq 0.1$ finite-volume schemes become unacceptable, the DG schemes work better and better. Calculations with $CFL = 0.01$ have shown that subsequent diminishing of CFL number leads to further growth of accuracy.

Fig.2,b compare basic schemes ($K=1$, Method 1)with the schemes with TVD method ($K=1$, Method 2) for $CFL = 0.1$ (i.e. $C_{\text{stab}} = 0.3$ for $K=1$). Use of the Method 2 increases the quality of results.

Figures 2,c,d demonstrates the influence of the grid step. In all cases, $CFL = 0.1$ (i.e. $C_{\text{stab}} = 0.3$ for $K=1$ and $C_{\text{stab}} = 0.4$ for $K=2$) and only scheme with TVD method (Method 2) was considered. For 2nd order scheme, we have results close to behavior of finite-volume scheme: acceptable results may be obtained only for 16 cells per wavelength. Doubling the grid step leads to crucial worsening the results. But 3rd order scheme allows to perform calculations even at 8 cells per wavelength without significant loss of quality.

The latter scheme - 3rd order DG scheme with TVD method ($K=2$, Method 2) may be recommended for acoustic applications.

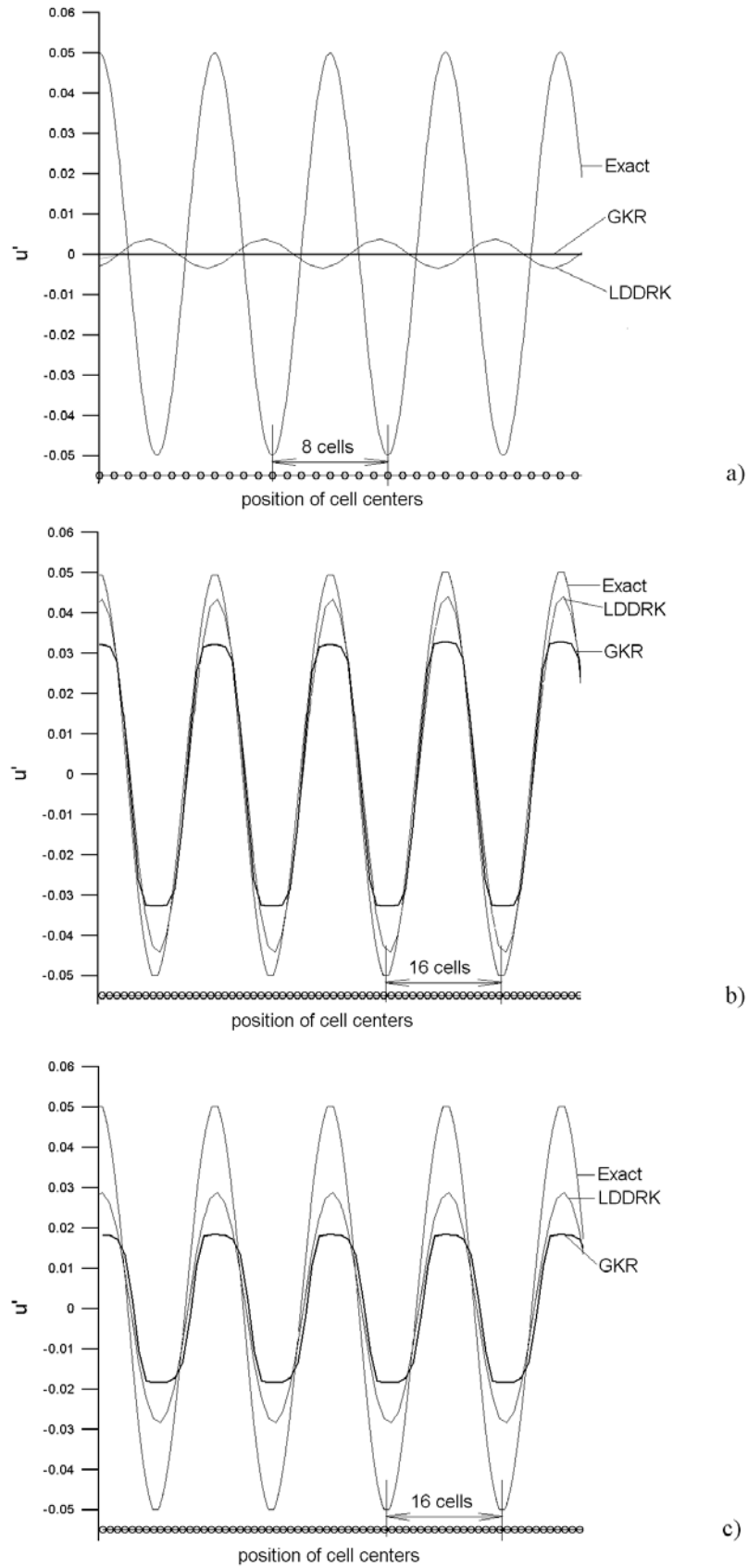


Figure 1. Dependence of solution upon grid step and upon stability coefficient for finite-volume schemes: a) 8 cells per wavelength, $C_{stab} = 0.5$; 16 cells per wavelength, $C_{stab} = 0.5$; c) 16 cells per wavelength, $C_{stab} = 0.1$

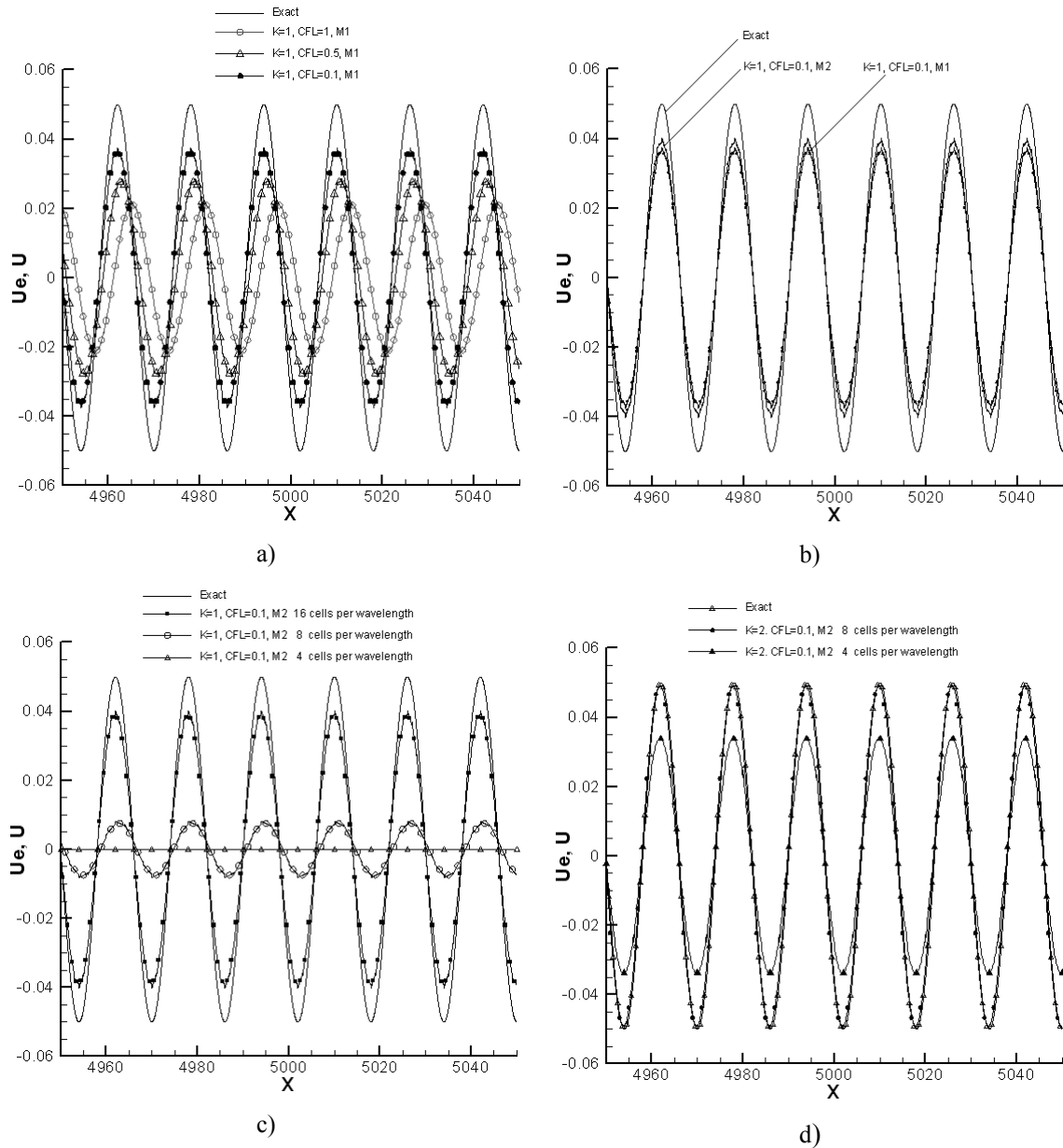


Figure 2. Dependence of solution upon scheme, grid step and upon stability coefficient for DG schemes:
 a) 16 cells per wavelength, CFL = 0.1; 0.5; 1, scheme $K = 1$, Method 1;
 b) 16 cells per wavelength, CFL = 0.1, scheme $K = 1$, Method 1 and Method 2;
 c) 16, 8 and 4 cells per wavelength, CFL = 0.1, scheme $K = 1$, Method 2;
 d) 16, 8 and 4 cells per wavelength, CFL = 0.1, scheme $K = 2$, Method 2

3. RIGOROUS FORMULATION OF ROE UPWIND APPROACH FOR LEE

Realization of Discontinuous Galerkin (DG) scheme for LEE, which is described in the previous Section, uses the upwind approach, which is based on solution of Riemann problem about decay of an arbitrary discontinuity.

We assume that flow near the boundary of computational cell has quasi-1D character: all gas parameters depend upon only two variables - (t, n) , where t is time and n is

coordinate along the normal to the boundary of computational cell $\vec{n} = (n_x, n_y, n_z)$. In the time moment $t = 0$ all gas parameters are continuous functions within each separate cell, but have discontinuities on the boundaries between neighboring cells. In this case, for determination of parameters at the cell boundary $n = n_0$ (n is coordinate along the \vec{n} direction) we may use the solution of classical self-similar Riemann problem about decay of an arbitrary discontinuity:

$$\begin{cases} \frac{\partial U}{\partial t} + \frac{\partial F_n}{\partial n} = 0, \\ U(n, 0) = \begin{cases} U^L, & n < n_0, \\ U^R, & n > n_0. \end{cases} \end{cases} \quad (12)$$

$$F_n(U(n_0, t)) = ?$$

An idea of Roe's approach⁷ to solution of problem (12) is to replace non-linear Euler equations by linearized system, using special-kind linearization of flux vector:

$$F_n(U) \approx \mathbf{A}U + C, \quad (13)$$

where constant matrix $\mathbf{A} = \mathbf{A}(U^L, U^R)$ and constant vector C should satisfy the following conditions:

$$\begin{cases} \mathbf{A}U^L + C = f(U^L), \\ \mathbf{A}U^R + C = f(U^R). \end{cases} \quad (14)$$

From (4.3) it follows that the matrix \mathbf{A} should satisfy the so-called “ Δ -condition”:

$$\mathbf{A} \cdot (U^R - U^L) = F_n(U^R) - F_n(U^L). \quad (15)$$

We may also impose additional condition: when discontinuity disappears ($U^L \rightarrow U^R$), matrix \mathbf{A} should tend to Jacobian of the flux $F_n(U)$:

$$\lim_{U^L, U^R \rightarrow U} \mathbf{A}(U^L, U^R) = \frac{\partial F_n}{\partial U}(U). \quad (16)$$

Linearization (13) allows to obtain analytical solution of Riemann problem (12). Let's represent $\mathbf{A} = \mathbf{P} \mathbf{\Lambda} \mathbf{P}^{-1}$, where $\mathbf{\Lambda} = \text{diag}(\lambda_i)$ - diagonal matrix of eigenvalues of \mathbf{A} , and $\mathbf{P} = \text{col}(e_i)$ - matrix of eigenvectors of \mathbf{A} (i -th column is eigenvector e_i , corresponding to eigenvalue λ_i). Eigenvalues of \mathbf{A} determine the characteristic lines $\frac{dn}{dt} = \lambda_i$. Along characteristics $\frac{dn}{dt} = \lambda_i$, Riemann invariant z_i is constant ($z = \mathbf{P}^{-1}U$). We have two sets of Riemann invariants, corresponding to states from the left and right sides of the discontinuity - $z^L = \mathbf{P}^{-1}U^L$ and $z^R = \mathbf{P}^{-1}U^R$. Let's consider the differences of invariants: $\Delta z_i \equiv z_i^R - z_i^L$. Then the solution of (12) may be represented as follows:

$$F_n(U(n_0, t)) = F_n(U^L) + \sum_{\lambda_i < 0} \Delta z_i \lambda_i e_i. \quad (17)$$

The only problem is to find matrix \mathbf{A} , which satisfies to conditions (15), (16).

It easy to show that for the full (non-linearized) Euler equations $\frac{\partial F_n(\mathbf{U})}{\partial \mathbf{U}}$ depends upon four independent variables: $(u; v; w; H)$. Roe⁷ have proposed to take $\mathbf{A}(\mathbf{U}^L, \mathbf{U}^R) = \frac{\partial F_n}{\partial \mathbf{U}}(\hat{u}, \hat{v}, \hat{w}, \hat{H})$ - Jacobian of flux $F_n(\mathbf{U})$, in which specially-averaged values are substituted. As a result, condition (16) is satisfied automatically. Roe have shown that for full non-linear Euler equations the following averagings may be used to satisfy (15):

$$\hat{\alpha} = \frac{\sqrt{\rho^L} \alpha^L + \sqrt{\rho^R} \alpha^R}{\sqrt{\rho^L} + \sqrt{\rho^R}}, \quad \alpha = u; v; w; H. \quad (18)$$

For Linearized Euler equations, Jacobian coincides with Jacobian of full Euler equations for unperturbed solution: $\frac{\partial F'_n(\mathbf{U}', \mathbf{U}_a)}{\partial \mathbf{U}'} \equiv \frac{\partial F_n(\mathbf{U}_a)}{\partial \mathbf{U}}$. Nevertheless, structure of LEE fluxes differs from the structure of fluxes for full Euler equations, condition (15) has also another structure, and Roe averagings (18) don't give matrix satisfying to (15). In any way, we should find another way to construct the Roe upwind approach for LEE.

Flux of full Euler equations may be represented as follows:

$$F_n(\mathbf{U}) = F_n(\mathbf{U}_a) + F'_n(\mathbf{U}', \mathbf{U}_a) + O(U'^2) = F_{an} + F'_n + O(U'^2), \quad (19)$$

where symbol $O(U'^2)$ denotes various nonlinear combinations of the vector \mathbf{U}' components. We have introduced designations: $F_n(\mathbf{U}_a) = F_{an}$, $F'_n(\mathbf{U}', \mathbf{U}_a) = F'_n$. For LEE, we may neglect $O(U'^2)$. Therefore, we have

$$F'_n(\mathbf{U}', \mathbf{U}_a) \approx F_n(\mathbf{U}) - F_n(\mathbf{U}_a) = F_n - F_{an}. \quad (20)$$

Formula (20) shows us the rational way to obtain the Roe approximation of the LEE conservative variables $\mathbf{U}'(n_0, t)$ and corresponding flux $F'_n(n_0, t)$. We should solve *two* Riemann problems:

1. Riemann problem (12) for full variables $\mathbf{U} = \mathbf{U}_a + \mathbf{U}'$:

$$\left\{ \begin{array}{l} \frac{\partial \mathbf{U}}{\partial t} + \frac{\partial F_n(\mathbf{U})}{\partial n} = 0, \\ \mathbf{U}(n, 0) = \begin{cases} \mathbf{U}_a^L + (\mathbf{U}')^L, & n < n_0, \\ \mathbf{U}_a^R + (\mathbf{U}')^R, & n > n_0. \end{cases} \end{array} \right. \quad (21)$$

$$\underline{F_n(\mathbf{U}(n_0, t)) = ?}$$

Solution of (21) will give us the values $\mathbf{U}(n_0, t)$ and corresponding flux $F_n(n_0, t)$.

2. Riemann problem (12) for unperturbed variables \mathbf{U}_a :

$$\begin{cases} \frac{\partial U}{\partial t} + \frac{\partial F_n(U)}{\partial n} = 0, \\ U(n,0) = \begin{cases} U_a^L, & n < n_0, \\ U_a^R, & n > n_0. \end{cases} \end{cases} \quad (22)$$

$$F_n(U(n_0, t)) = ?$$

Solution of (22) will give us the values $U_a(n_0, t)$ and corresponding flux $F_{an}(n_0, t)$.

Finally, we may take

$$F'_n(n_0, t) = F_n(n_0, t) - F_{an}(n_0, t). \quad (23)$$

For solutions of problems (21) and (22), we may use Roe approximation (17).

Solution of Riemann problem (21) for full variables $U = U_a + U'$:

$$F_n(n_0, t) = F_n(U^L) + \sum_{\lambda_i < 0} \Delta z_i \lambda_i e_i, \quad (24)$$

where λ_i and e_i - eigenvalues and eigenvectors of the Roe matrix $A(U^L, U^R)$, and $\Delta z_i = \mathbf{P}^{-1}(U^R - U^L)$, $\mathbf{P} = \text{col}(e_i)$. In the framework of Roe approach, $A(U^L, U^R) = \frac{\partial F_n}{\partial U}(\hat{u}, \hat{v}, \hat{w}, \hat{H})$, where

$$\hat{\alpha} = \frac{\sqrt{(\rho_a + \rho')^L} \cdot (\alpha_a + \alpha')^L + \sqrt{(\rho_a + \rho')^R} \cdot (\alpha_a + \alpha')^R}{\sqrt{(\rho_a + \rho')^L} + \sqrt{(\rho_a + \rho')^R}}. \quad (25)$$

Solution of Riemann problem (22) for unperturbed variables U' :

$$F_{an}(n_0, t) = F_n(U_a^L) + \sum_{\lambda_{ai} < 0} \Delta z_{ai} \lambda_{ai} e_{ai}, \quad (26)$$

where λ_{ai} and e_{ai} - eigenvalues and eigenvectors of *another* Roe matrix - $A(U_a^L, U_a^R)$, and $\Delta z_{ai} = \mathbf{P}_a^{-1}(U_a^R - U_a^L)$, $\mathbf{P}_a = \text{col}(e_{ai})$. In the framework of Roe approach, $A(U_a^L, U_a^R) = \frac{\partial F_n}{\partial U}(\hat{u}_a, \hat{v}_a, \hat{w}_a, \hat{H}_a)$, where

$$\hat{\alpha}_a = \frac{\sqrt{\rho_a^L} \cdot \alpha_a^L + \sqrt{\rho_a^R} \cdot \alpha_a^R}{\sqrt{\rho_a^L} + \sqrt{\rho_a^R}}. \quad (27)$$

Substituting (24) and (26) into (23) and using approximation $F'_n(U'^L) \approx F_n(U^L) - F_n(U_a^L)$ (i.e. neglecting $O(U'^2)$ again), we shall obtain Roe upwind approximation for LEE flux:

$$F'_n(n_0, t) = F'_n(U'^L) + \sum_{\lambda_i < 0} \Delta z_i \lambda_i e_i - \sum_{\lambda_{ai} < 0} \Delta z_{ai} \lambda_{ai} e_{ai}. \quad (28)$$

It is worth to add that the term $\sum_{\lambda_{ai} < 0} \Delta z_{ai} \lambda_{ai} e_{ai}$ in formula (28) may be calculated once, at the beginning of calculation, for all boundaries of all cells, and may be stored in the memory. In this case, quantity of arithmetical operations during the calculation will be close to single solution of the Riemann problem.

4. ANALYSIS OF POSSIBLE SIMPLIFICATIONS

Rigorous formulation of Roe upwind approach for LEE, which was described in the previous section, is rather complicated. It requires to solve 2 Riemann problems and contains rather bulky formulas. But Linearized Euler Equations are written for the case of small perturbations of gas parameters, and this fact gives us possibility to simplify all formulas. Now we shall consider possible simplifications of this approach with the aim to minimize computational cost of this procedure.

First possible simplification: using single solution of Riemann problem for LEE with approximate Roe matrix. Necessity to solve two Riemann problems for LEE is connected with the fact that we don't know the exact Roe matrix for LEE, but know exact Roe matrix for full (unperturbed) Euler equations. If the exact Roe matrix for LEE would be known, we may to solve only one Riemann problem directly for LEE.

Let's consider the possibility to take $\mathbf{A} = \frac{\partial F_n}{\partial U}(\hat{u}, \hat{v}, \hat{w}, \hat{H})$ - Jacobian of the full Euler flux $F_n(U)$, in which the Roe averages of *aerodynamic solution* (27) are substituted.

This way to calculate Roe matrix for LEE is approximate, simplified approach. *Resulting matrix is not exact Roe matrix for the LEE flux:* it doesn't satisfy to Roe's "delta" condition $F'_n((U')^R, U_a^R) - F'_n((U')^L, U_a^L) = \mathbf{A} \cdot ((U')^R - (U')^L)$.

To check the possibility of such simplification, we have calculated the value $\mathbf{A} \cdot ((U')^R - (U')^L) - [F'_n((U')^R, U_a^R) - F'_n((U')^L, U_a^L)]$ for the case of 1D flow. The result was following. For the fluxes of density fluctuations, Roe's "delta" condition is satisfied, and this difference is equal to zero. But for the fluxes of momentum fluctuations and energy fluctuations, this is not so. Here we shall only show the result for the flux of momentum fluctuations:

$$\begin{aligned} & \left\{ \mathbf{A} \cdot ((U')^R - (U')^L) - [F'_n((U')^R, U_a^R) - F'_n((U')^L, U_a^L)] \right\}_2 = \\ & = \frac{3-\gamma}{2} \cdot (u_a^R - u_a^L)^2 \cdot \frac{\rho_a^R \rho_a^{L'} - \rho_a^L \rho_a^{R'}}{(\sqrt{\rho_a^R} + \sqrt{\rho_a^L})^2} - \\ & - (3-\gamma) \cdot (u_a^R - u_a^L) \cdot \sqrt{\rho_a^R \cdot \rho_a^L} \cdot \frac{(\rho_a^L + \sqrt{\rho_a^L \cdot \rho_a^R}) \cdot u'^L + (\rho_a^R + \sqrt{\rho_a^L \cdot \rho_a^R}) \cdot u'^R}{(\sqrt{\rho_a^R} + \sqrt{\rho_a^L})^2}. \end{aligned} \quad (29)$$

In the case of correct Roe matrix, this difference should be equal to zero. Its diversity from zero is an error in approximation of flux.

For the comparison, let's consider the flux of momentum fluctuation itself:

$$[F'_n(U', U_a)]_2 = (\rho_a \cdot u' + u_a \cdot \rho') \cdot u_a + \rho_a u_a \cdot u' + p'. \quad (30)$$

It is easy to see: if $u_a^R - u_a^L \sim u_a$, then the second term of the error (29) is comparable with the value of flux itself (30). Condition $u_a^R - u_a^L \sim u_a$ is satisfied in the case of fast variation of basic (aerodynamic) flowfield, - especially across shocks.

Second possible simplification: using primitive variables $Q' = (\rho', u', v', w', p')^T$
instead of conservative variables $U' = [\rho'; (\rho u)'; (\rho v)'; (\rho w)'; (\rho E)']^T$.

Roe's solution of Riemann problem (17) may also be rewritten in symmetrical form:

$$F_n(n_0, t) = \frac{F_n^L + F_n^R}{2} - |\mathbf{A}| \frac{\Delta U}{2}, \quad (31)$$

where $\Delta U = U^R - U^L$. \mathbf{A} is Roe matrix. If we represent $\mathbf{A} = \mathbf{P} \mathbf{\Lambda} \mathbf{P}^{-1}$, then $|\mathbf{A}| = \mathbf{P} |\mathbf{\Lambda}| \mathbf{P}^{-1}$, where $|\mathbf{\Lambda}|$ is diagonal matrix containing modules of eigenvalues of the matrix \mathbf{A} .

Transition to primitive variables Q may be realized using the following relation:

$$dU = \Gamma dQ. \quad (32)$$

Here $\Gamma = \frac{\partial U}{\partial Q}$. Replacing *approximately* in (32) differentials by finite differences, we may write $\Delta U \approx \Gamma \Delta Q$.

Now we may compare computational cost of both approaches.

In Conservative Variables Approach, we should calculate the following product of matrices and vectors:

$$\mathbf{P} \cdot |\mathbf{\Lambda}| \cdot \mathbf{P}^{-1} \cdot \Delta U. \quad (33)$$

In Primitive Variables Approach, we should calculate the following product:

$$\mathbf{P} \cdot |\mathbf{\Lambda}| \cdot \mathbf{L}^{-1} \cdot \Delta Q, \quad (34)$$

where $\mathbf{L}^{-1} \equiv \mathbf{P}^{-1} \cdot \Gamma$. But for Euler equations, matrix \mathbf{L}^{-1} and vector ΔQ are much simpler and more compact than matrix \mathbf{P}^{-1} and vector ΔU , respectively. As a result, (34) requires much less arithmetical operations than (33).

But it is necessary to remember that transition from (33) to (34) is connected with errors, produced by replacement of differentials by finite differences. As a result, substitution of (34) in (31) instead of (33) will result in additional errors in Roe's linearized solution of Riemann problem. Error of Primitive Variable Approach may be defined as $\varepsilon \equiv \mathbf{P} \cdot |\mathbf{\Lambda}| \cdot \mathbf{P}^{-1} \cdot \Delta U - \mathbf{P} \cdot |\mathbf{\Lambda}| \cdot \mathbf{L}^{-1} \cdot \Delta Q$ (see (31) and (34)). This error may be

compared with the value of flux f itself. We have performed this comparison for 1D case, when ε is vector of 3 components (ε_1 is error in flux of mass, ε_2 - in flux of momentum, ε_3 - in flux of energy.) We shall show here only ε_2 :

$$\begin{aligned} \varepsilon_2 = & 2\hat{u} \cdot \underbrace{[\Delta(\rho_a u') - \hat{\rho} \cdot \Delta u']}_{O(u_a u' \cdot \Delta \rho_a)} + (\gamma - 1) \cdot \underbrace{[\Delta(\rho_a u_a u') - \hat{u} \cdot \Delta(\rho_a u')]}_{O(\rho_a u' \cdot \Delta u_a)} + \\ & + (3 - \gamma) \cdot \underbrace{\hat{u} \cdot [\Delta(u_a \rho') - \hat{u} \cdot \Delta \rho']}_{O(u_a \rho' \cdot \Delta u_a)} + \frac{\gamma - 1}{2} \cdot \underbrace{[\Delta(u_a^2 \rho') - \hat{u}^2 \cdot \Delta \rho']}_{O(\rho' \cdot \Delta u_a^2)} \end{aligned} \quad (35)$$

Comparison of (35) with the expression for the flux of momentum itself (30) shows that Primitive Variables Approach is applicable, only if $|\Delta \sigma_a| = |(\sigma_a)_R - (\sigma_a)_L| \ll |\sigma_a|$, where $\sigma = \rho; u; p$. In particular, variant $|\Delta \sigma_a| = O(\sigma')$ is acceptable. It should be pointed that we have obtained the same requirement for the first simplification. Therefore, Primitive Variables Approach and single solution of Riemann problem for LEE with approximate Roe matrix may be used together.

If we have slowly varying aerodynamic field ($|\Delta \sigma_a| = |(\sigma_a)_R - (\sigma_a)_L| \ll |\sigma_a|$) and use Primitive Variables Approach together with single solution of Riemann problem for LEE with approximate Roe matrix, then **the third simplification** may be made: **we may replace Roe averagings (4.21) by simple arithmetic mean:**

$$\hat{\alpha} = \frac{\alpha^L + \alpha^R}{2}, \quad \alpha = u; v; w; H. \quad (36)$$

The last improvement in the speed of calculations may be made, if we shall perform calculations on the basis of Isentropic Linearized Euler Equations (ILEE). This is simplified equation system, which may be obtained from full Linearized Euler Equations (LEE), if we replace the last differential equation (equation for energy) by isentropic relation $p' = c_a^2 \cdot \rho'$. For ILEE, $Q' = (\rho', u', v', w')^T$, and flux of Q' per unit area in direction of the vector $\vec{n} = (n_x, n_y, n_z)$ is equal to

$$F'_n \equiv \vec{F}'(U', U_a) \cdot \vec{n} = \begin{pmatrix} D'_n \\ u_a D'_n + \rho_a V_{an} u' + n_x c_a^2 \rho' \\ v_a D'_n + \rho_a V_{an} v' + n_y c_a^2 \rho' \\ w_a D'_n + \rho_a V_{an} w' + n_z c_a^2 \rho' \end{pmatrix}. \quad (37)$$

Isentropic LEE not only includes smaller quantity of partial differential equations, but provides essentially simpler form of all relations.

5. EXAMPLE OF TEST TASK SOLUTION

To demonstrate operability of the proposed DG schemes with TVD Runge-Kutta time integration and with simplified Roe solver for isentropic LEE, they were applied to test task about development of Gaussian acoustic pulse in a uniform flow.

This test task is described in the paper⁸. In the same paper, analytical solution is given. Analogous 2D and 3D problems were considered during Second Computational Aeroacoustics Workshop on Benchmark Problems (CAA-2)⁹.

Structure of initial field and initial distribution of pressure fluctuation are shown in Fig.3.

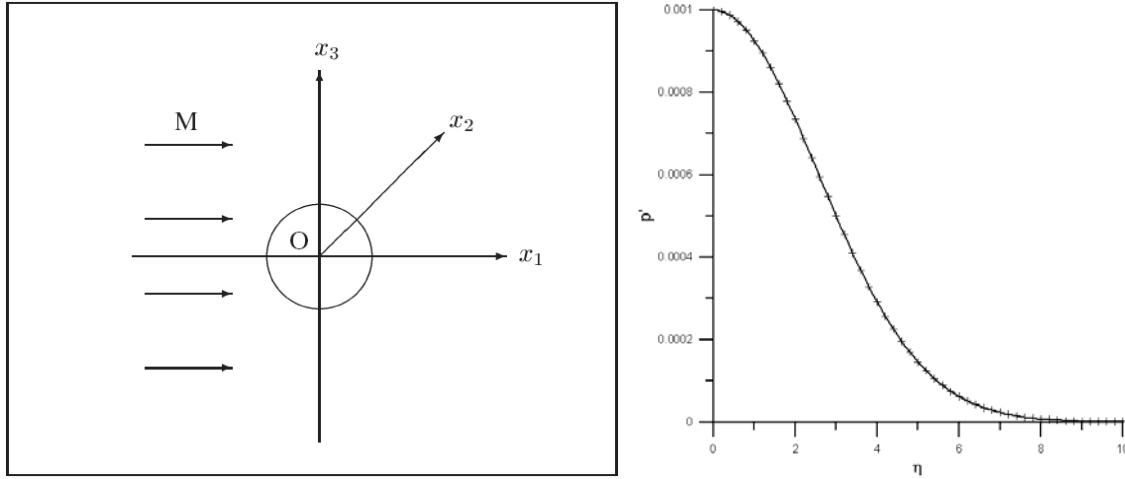


Figure 3. Initial field for the task about Gaussian pulse

Aerodynamic field in this test task is stationary uniform flow:

$$\begin{cases} p_a = \frac{1}{\gamma}, & \rho_a = 1 \quad (\Rightarrow c_a = \sqrt{\gamma \frac{p_a}{\rho_a}} = 1), \\ u_a = M_a = 0.5, & v_a = w_a = 0. \end{cases} \quad (38)$$

At the initial time moment, Gaussian acoustic pulse is introduced:

$$\begin{cases} p' = \varepsilon \cdot \exp[-\alpha(x^2 + y^2 + z^2)] \\ \rho' = p' / c_a^2 = p', \\ u' = v' = w' = 0, \end{cases} \quad (39)$$

where $\varepsilon = 10^{-3}$ - amplitude, $\alpha = \frac{\ln 2}{b^2}$, $b = 3$ - Gaussian half-width (for $\sqrt{x^2 + y^2 + z^2} = b$, $p' = \varepsilon / 2$).

This test task has exact analytical solution⁸:

$$p'(\eta, t) = \frac{\varepsilon}{\beta} \int_0^\infty \xi^2 \exp\left[-\frac{\xi^2}{4\alpha}\right] \cos(\xi t) \frac{\sin(\xi \cdot |\eta|)}{\xi \cdot |\eta|} d\xi, \quad (40)$$

where $\eta = \text{sgn}(x - M_a t) \cdot \sqrt{(x - M_a t)^2 + y^2 + z^2}$, $\beta = 2\alpha\sqrt{\pi\alpha}$.

In our tests, we have used cubical **computational domain** ($\underbrace{[-50; 50]}_x \times \underbrace{[-50; 50]}_y \times \underbrace{[-50; 50]}_z$), covered by uniform square grid. Solution was considered in the moment $t = 20$. On the basis of Discontinuous Galerkin (DG)

approach for Isentropic Linearized Euler Equations (ILEE), four calculations were performed:

1. 2nd order DG scheme (K=1) with TVD method, 50 cells in each spatial direction.
2. 3rd order DG scheme (K=2) with TVD method, 37 cells in each spatial direction (the same number of freedom degrees (NDOF) as in 50-cells calculation using DG K=1 scheme).
3. 2nd order DG scheme (K=1) with TVD method, 90 cells in each spatial direction.
4. 3rd order DG scheme (K=2) with TVD method, 66 cells in each spatial direction (the same value of NDOF as in 90-cells calculation using DG K=1 scheme).

“Number of degrees of freedom” (NDOF) in DG is quantity of independent variables per each gas parameter in each computational cell. For the case of DG scheme with K=1, NDOF = 4. For the case K=2, NDOF = 10. It is usual approach in DG methods – to compare different schemes at the same total NDOF for all cells of computational domain. Therefore, quantity of cells N_{cells} in calculations on the basis K=1 and K=2 schemes should satisfy the following condition:

$$(N_{\text{cells}} \cdot \text{NDOF})_{DG\ K=1} = (N_{\text{cells}} \cdot \text{NDOF})_{DG\ K=2}. \quad (41)$$

In our case, $N_{\text{cells}} = N_x^3$, where N_x is quantity of cells in each spatial direction. Therefore, we have the following requirement:

$$(N_x)_{DG\ K=1} \cdot \sqrt[3]{4} = (N_x)_{DG\ K=2} \cdot \sqrt[3]{10}. \quad (5.4)$$

Results for the moment $t = 20$ (distribution $p'(\eta)$ along x -axis) and their comparison with exact solution are shown in Figure 4. The worst solution was obtained in first calculation (K=1, $N_x = 50$) – see Fig.4,a. It is characterized by strong asymmetry in x -direction, by strong smoothing of the peaks and by essentially discontinuous character of reconstructed solution between the cell centers. It is interesting that numerical smoothing of pulse is higher in the right part of pulse, which propagates downstream. The best agreement with exact solution was achieved in fourth calculation (K=2, $N_x = 66$) – see Fig.4,b.

Comparison of first two calculations with K=1 and K=2 is performed in Fig.4,c (right part of the pulse). Analogous comparison of third calculation (K=1, 90 cells) and fourth calculation (K=2, 66 cells) is performed in Fig.4,d. Naturally, in calculations 3 and 4 results are better, and solutions with K=1 and K=2 are more close to each other.

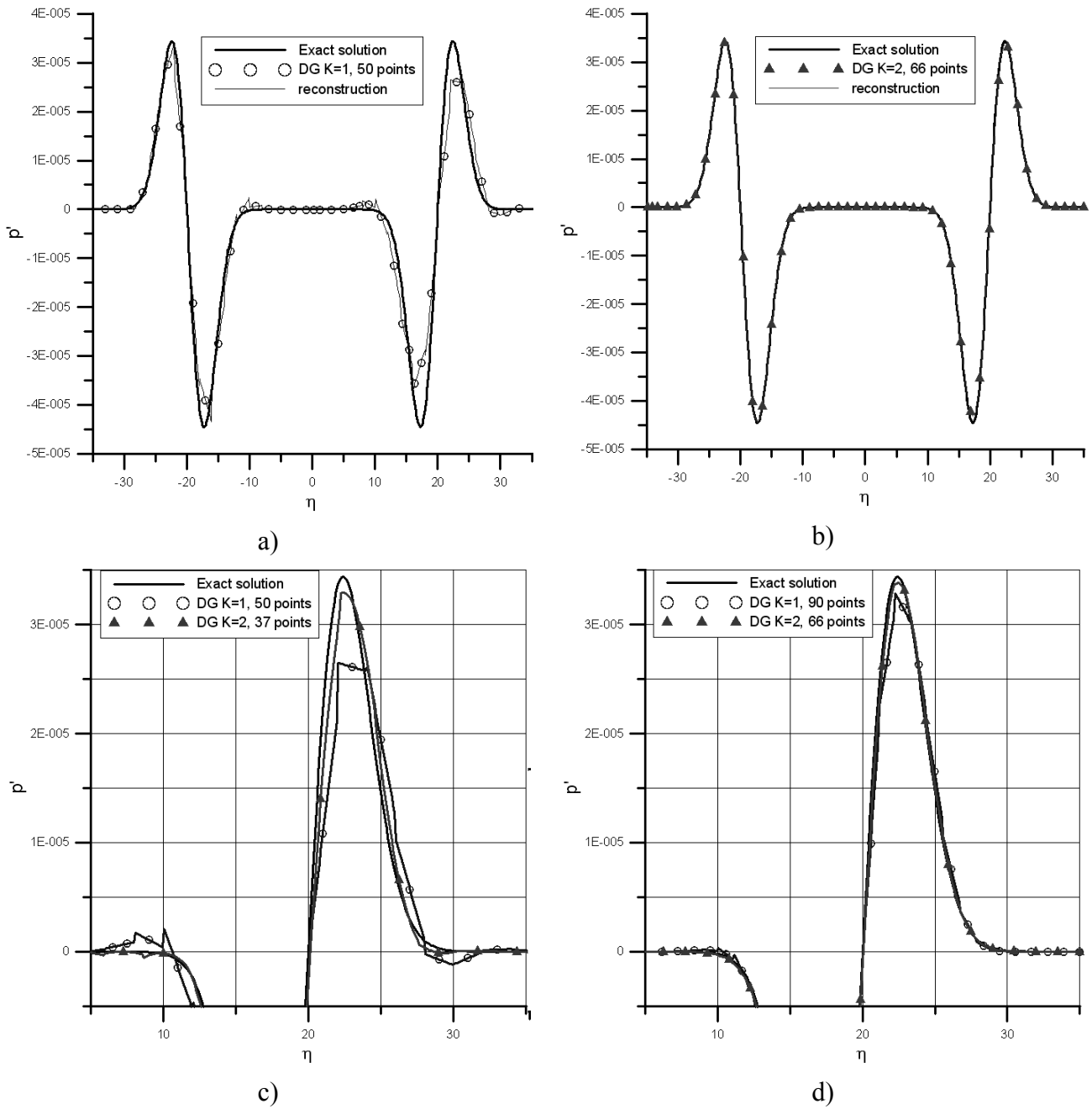


Figure 4. Computed distributions of pressure fluctuations along x-axis for the moment $t=20$ and their comparison with exact solution: a) full distribution for the worst solution; b) full distribution for the best solution; c) details for the coarse grid, $K=1$ and $K=2$; d) details for the fine grid, $K=1$ and $K=2$

6. CONCLUSIONS

1. 3rd order DG scheme with TVD method may be recommended for acoustic applications. This scheme allows calculations on grid with 8 cells per wavelength.

2. Contrary to finite-volume schemes, quality of results for DG schemes increases with diminishing of CFL number. For 1D test task, good results were obtained in calculations with $CFL < 0.1$.

3. If the aerodynamic field is varied slowly (for each aerodynamic parameter $|\Delta\sigma_a| = |(\sigma_a)_R - (\sigma_a)_L| \ll |\sigma_a|$), then Roe upwind approach for LEE may be essentially simplified: it is possible to use the same Roe matrix as for full Euler equations, to replace Roe averagings by simple arithmetic mean and to use primitive variables instead of conservative variables. Due to these simplifications, the computational effectiveness of Roe upwind approach increases essentially in comparison with rigorous formulation. But if aerodynamic flow varies quickly, errors of simplified formulation may be comparable with LEE fluxes.

7. REFERENCES

- [1] B. Cokburn. “Discontinuous Galerkin methods for convection-dominated problems”, in *High-Order Methods for Computational Physics*, edited by T. Barth and H. Deconik, Lecture Notes in Computational Science and Engineering, Springer Verlag, Berlin, Vol. 9, pp. 69-224 (1999).
- [2] *Third Computational Aeroacoustics (CAA) Workshop on Benchmark Problems (Cleveland, Ohio, November 8–10, 1999)*. NASA Glenn Research Center, NASA/CP—2000-209790 (2000).
- [3] *Fourth Computational Aeroacoustics (CAA) Workshop on Benchmark Problems (Brook Park, Ohio, October 20–22, 2003)*. NASA Glenn Research Center, NASA/CP—2004-212954 (2004).
- [4] H.L. Atkins. “Continued development of the Discontinuous Galerkin Method for computational aeroacoustic applications”. *NASA-AIAA-97-1581* (1997).
- [5] A.G. Kulikovskii, N.V. Pogorelov, A.Yu. Semenov. *Mathematical aspects of numerical solution of hyperbolic systems*. Monographs and Surveys on Pure and Applied Mathematics, Vol.188, Chapman and Hall/CRC, Boca Raton, FL. (2001).
- [6] C.K.W. Tam, J.C. Webb. “Dispersion-Relation-Preserving schemes for computational acoustics”, *Journal of Computational Physics*, Vol.107, pp. 262-281 (1993).
- [7] P.L. Roe. “Approximate Riemann solvers, parameter vectors, and difference schemes”. *Journal of Computational Physics*, Vol.43, pp.357-372 (1981).
- [8] C. Bogey, C. Bailly. “Three-dimensional non-reflective boundary conditions for acoustic simulations: far field formulation and validation test cases”. *ACTA ACUSTICA united with ACUSTICA*, Vol. 88, pp.463 – 471 (2002).
- [9] *Second Computational Aeroacoustics (CAA) Workshop on Benchmark Problems (November 4-5, 1996)*. Edited by C.K.W. Tam and J.C. Hardin. NASA Langley Research Center, *NASA Conference Publication 3352* (1997).